

Mapping the central parsec in M-band spectroscopy

Jihane Moultaqa*

IRAP, Observatoire Midi-Pyrénées, CNRS, Université Toulouse III, France

E-mail: jihane.moultaqa@irap.omp.eu

Andreas Eckart

I-Physikalisches Institut, Universität zu Köln, Germany

E-mail: eckart@ph1.uni-koeln.de

Nadeen Sabha

I-Physikalisches Institut, Universität zu Köln, Germany

E-mail: sabha@ph1.uni-koeln.de

We present the first spectroscopic datacube of the central parsec of our Galaxy in the M-band filter from 4.4 to 5.1 μm . The observations were done at the ESO-VLT telescope using the ISAAC spectrograph. Our data allowed us to map the solid ice ^{12}CO present locally in the central region as well as the gaseous CO that appears to be associated with the local environment (circumstellar and minispiral material). Our findings imply very low temperatures in the direct vicinity of the central Blackhole SgrA*.

Nuclei of Seyfert galaxies and QSOs - Central engine & conditions of star formation

6-8 November, 2012

Max-Planck-Institut für Radioastronomie (MPIfR), Bonn, Germany

*Speaker.

1. The observations

We used the ISAAC spectrograph located at the ESO UT3-VLT telescope in order to map the central parsec of our Galaxy in the M-band spectroscopic domain. We needed three periods of observations and 22 slit positions in order to map the desired region with a seeing varying from $0.4''$ to $1.5''$. This ended up with the first datacube of the region in the M-band of the spectrum (i.e. from $4.4 \mu\text{m}$ to $5.1 \mu\text{m}$). Because of technical problems, two slit positions were not observed during our runs. Therefore, we interpolated the spectra at these positions. Moreover, in six other slit positions we were not able to remove the sky properly but we made sure that the measurements we derived from our cube were not affected by the sky emission lines.

2. Correcting the line of sight extinction

2.1 The solid ice ^{12}CO line

In [4], we derived a spectrum of the foreground contribution from the solid-phase ^{12}CO absorption line located at $4.675 \mu\text{m}$ (see Fig. 6(a) and explanation in that paper). We showed that this spectrum diluted with an additional continuum of about 4 Jy is well suited to describe the foreground overall extinction in the spectral region.

Here we derive a corrected datacube for the foreground extinction by dividing the whole cube with the previous spectrum diluted by a 4 Jy continuum. The resulting integrated smoothed map is shown in Fig. 1 (left).

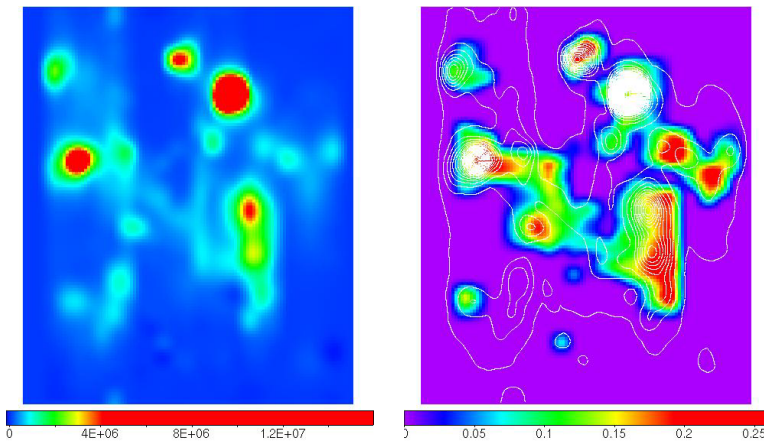


Figure 1: *Left:* Smoothed M-band continuum map of the central half parsec of our Galaxy. *Right:* The gaseous $^{13}\text{CO-R}(0)$ optical depth map of the central half parsec obtained after correcting the datacube for the solid ^{12}CO foreground extinction line. We overplot in white contours of the continuum map.

2.2 The gaseous $^{13}\text{CO-R}(0)$ line

From the non-corrected and corrected datacubes for the foreground extinction we constructed the optical depth maps of the gaseous $^{13}\text{CO-R}(0)$ line (located at $4.765 \mu\text{m}$). The extinction corrected map is shown in Fig. 1 (right). In order to measure the optical depths τ , we considered the

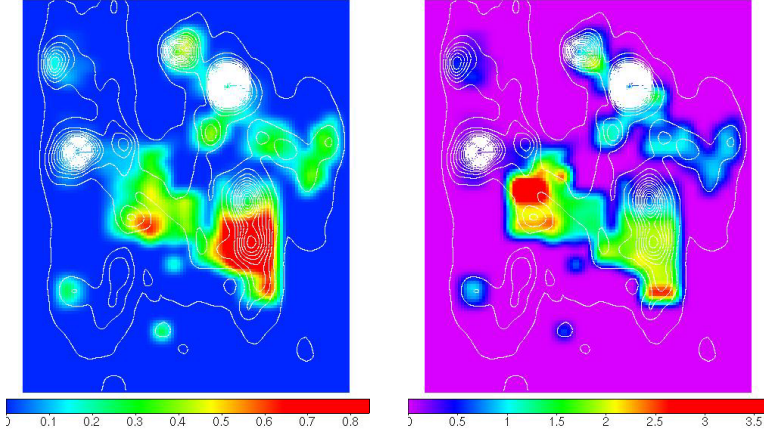


Figure 2: *Left:* Optical depth map of the ^{12}CO solid line corrected for the foreground extinction due to the same line. This map shows the residuals. *Right:* Map of the optical depth ratio of the solid ^{12}CO to gaseous $^{12}\text{CO-P}(2)$ line corrected for the foreground ^{12}CO line contribution. Contours of the continuum map are also overplotted.

continuum as a straight line connecting the spectra from $4.58\ \mu\text{m}$ to $4.8\ \mu\text{m}$ and the line intensity at $4.765\ \mu\text{m}$. The optical depth is then derived from the definition:

$$\tau = -\ln(I_{\text{continuum at } 4.765\ \mu\text{m}}/I_{\text{line at } 4.765\ \mu\text{m}}).$$

In these maps, we interpolated the optical depth values at the locations of the slit positions contaminated by the sky emission lines. The optical depths were derived at spatial pixels where the signal to noise in the integrated map was higher than about 10.

The resulting maps agree well with our previous work presented in [4] on individual sources of the Galactic Center. We find roughly the same values of the optical depths at the locations of the sources. For IRS 16C, we find a value of about 0.1 in the corrected map which was the value we used in that paper to correct all the spectra for the gaseous foreground absorption. Indeed, IRS 16C is an early-type star located outside the minispiral material made of ionized gas and dust, it is thus a perfect candidate which spectrum can be considered as free from local (circumstellar and interstellar medium) gaseous ^{13}CO absorption line. Therefore, this absorption line observed in the spectrum of IRS 16C is considered to arise from the line of sight material.

Correcting the map for this foreground gaseous ^{13}CO line provides a similar map than that of Fig. 1 with values of the optical depths reduced by 0.1. This residual ^{13}CO gas is likely to be associated with the circumstellar or interstellar local material.

This is in agreement with masses of circumstellar shells derived in the Galactic Center and based on published hydrogen number density estimates from sub-millimeter CO(7-6) and FIR [OI] line data, that we found to be of the order of $10^3 - 10^2\ M_{\odot}$.

3. The solid-phase ^{12}CO residual line

Since the continuum used to derive the optical depths of the $^{13}\text{CO-R}(0)$ absorption line gave results that agree well with our previous work, we can trust this first approximation continuum in

order to derive optical depth maps of the solid-phase ^{12}CO line.

The line intensity is taken at $4.675\ \mu\text{m}$ and the continuum intensity is that of the continuum at the same wavelength. In these maps, the optical depths are also derived at pixels where the integrated M-band map has a signal-to-noise ratio higher than 7.

In Fig. 2 (left), we show the smoothed map of the optical depths obtained from the extinction corrected datacube. We find residuals of the solid ^{12}CO line with optical depth values ranging from 0.1 to 0.9. This is to compare with the foreground contribution which is about 0.1-0.2 (see [4]).

A large amount of residuals is found in the IRS 13, IRS 2 region (even though two slit positions were interpolated in this area). These high optical depth values can be due to the gaseous $^{12}\text{CO-P}(1)$ line which is located at the same wavelength (see Fig. 8 of [4] showing the theoretical spectrum published by Moneti et al. (2001) and plotted at our spectral resolution). In that figure, we measure the ratio between the optical depths of the $^{12}\text{CO-P}(1)$ and the $^{12}\text{CO-P}(2)$ lines and find a value of 1.05. We can thus compare the same ratio in our maps with this value and conclude that if this ratio is higher than 1.05, then there is a residual solid-phase ^{12}CO line.

In Fig. 2 (right), we show the optical depth ratio map of the solid ^{12}CO to gaseous $^{12}\text{CO-P}(2)$ line corrected for the foreground ^{12}CO line contribution. In this map, we can see clearly that the ratio is much higher than 1.05, especially in the southern and western parts of the maps.

4. Conclusion

Our data shows large quantities of solid ^{12}CO in the local environment implying very low temperatures of less than 60 K in the central parsec surrounding the supermassive Black Hole Sgr A*. We show in [4], that the presence of bow shock sources (e.g., [8], [9]), narrow dust filaments ([5]; [7];[1]), and dust-embedded YSOs (IRS 13N; [6]) suggest the presence of high-density pockets and high-optical depths. At such high optical depths, gas temperatures can fall below the dust temperatures of 200 K on average in the minispiral. This is also stressed by the presence of water ices in the central parsec as we already showed in [2], [3].

References

- [1] Morris & Maillard 2000, ASP Conf ser. 195
- [2] Moutaka et al. 2004, A&A 425
- [3] Moutaka et al. 2005, A&A 443
- [4] Moutaka J., Eckart, A. et al. 2009, ApJ, 703
- [5] Muzic et al. 2007, A&A 469
- [6] Muzic et al. 2008, A&A 482
- [7] Paumard et al. 2001, A&A 366
- [8] Tanner et al. 2002, ApJ 575
- [9] Tanner et al. 2005, ApJ 624